

# Transition from a relativistic constituent-quark model to the quantum-chromodynamical asymptotics: a quantitative description of the pion electromagnetic form factor at intermediate values of the momentum transfer

S.V. Troitsky<sup>1</sup> and V.E. Troitsky<sup>2</sup>

<sup>1</sup>*Institute for Nuclear Research of the Russian Academy of Sciences,  
60th October Anniversary Prospect 7a, Moscow 117312, Russia\**

<sup>2</sup>*D.V. Skobeltsyn Institute of Nuclear Physics, M.V. Lomonosov Moscow State University, Moscow 119991, Russia<sup>†</sup>*  
(Dated: v.2: October 30, 2013)

We adopt a non-perturbative relativistic constituent-quark model for the  $\pi$ -meson electromagnetic form factor, which have successfully predicted experimental results, and supplement it with the effective momentum-dependent quark mass to study quantitatively the transition to the perturbative QCD asymptotics. The required asymptotical behaviour (including both the  $Q^{-2}$  fall-off and the correct coefficient) settles down automatically when the quark mass is switched off; however, the present experimental data on the form factor suggest that this cannot happen at the values of the momentum transfer below  $\sim 10 \text{ GeV}^2$ . The effective constituent-quark mass below this scale acquires substantial non-perturbative contributions.

PACS numbers: 13.40 Gp, 14.40 Be, 12.39 Ki, 11.10 Jj

## I. INTRODUCTION

Bound states of light quarks, and the  $\pi$  meson in particular, represent a challenging testbed for our understanding of the strong interaction. Theoretical approaches to their description are split into two directions. From the high-energy side, the quantum chromodynamics (QCD), which is widely believed to be a fundamental theory of the strong force, becomes strongly coupled at the relevant energy scales, so trustable perturbative calculations help a little in quantitative description of precise low-energy data, which there is no lack of. From the low-energy side, a number of successful models to describe the data have been developed. To be quantitative, they necessarily require some phenomenological input. None of these models can be consistently and quantitatively derived from the QCD lagrangian, therefore a gap between the two approaches emerges. The purpose of the present paper is to contribute to filling this gap by making a bridge between a successful low-energy model and the high-energy QCD calculation. We choose the electromagnetic form factor of the charged pion as the observable to study.

While most of the approaches fall into one of two groups, that is either low-energy (soft) or high-energy (hard) ones, and therefore cannot address the intermediate (transition) range of typical energies or momenta, there are some remarkable attempts to cover all energy scales within a single framework. One is the numerical non-perturbative QCD realized at the lattice. Despite

a considerable success, technical difficulties presently prevent it from obtaining reliable quantitative results for light mesons at intermediate momenta. Another approach is based on the holographic duality between strongly and weakly coupled theories which, for QCD, has not been rigorously proven, though works well in a number of phenomenological applications. By definition, any duality construction is uneasy to implement quantitatively at intermediate energies, where both dual theories are moderately strongly coupled.

Our goal here is less ambitious. We adopt frameworks of a particular relativistic constituent-quark model with low-energy phenomenological parameters included and study how the QCD asymptotics is reached within this particular model.

The asymptotics of the pion electromagnetic form factor  $F_\pi$  at momenta transfer  $Q^2 \rightarrow \infty$  has been determined [1–3], in the QCD frameworks, as

$$Q^2 F_\pi(Q^2) \rightarrow 8\pi\alpha_s^{1-\text{loop}}(Q^2) f_\pi^2, \quad (1)$$

where  $\alpha_s^{1-\text{loop}}(Q^2) = 4\pi/(\beta_0 \log(Q^2/\Lambda_{\text{QCD}}^2))$  is the one-loop running strong coupling constant,  $\beta_0 = 11 - 2N_f/3$  is the first beta-function coefficient,  $N_f$  is the number of active quark flavours and  $f_\pi \approx 130 \text{ MeV}$  [4] is the pion decay constant. It is important to note that this asymptotical behaviour, consistent with the quark counting rules [5, 6], includes the one-loop coupling only and is to be modified whenever the one-loop approximation fails, but not by means of a simple replacing of  $\alpha_s$  with its more precise value. Involved QCD calculations have been performed to obtain corrections to Eq. (1), see e.g. [7]. The QCD does not predict the value of  $Q^2$  at which this asymptotics should be reached.

On the other hand, the experimental data on  $F_\pi$  (see e.g. Ref. [8] for a review) are well described by a num-

\* st@ms2.inr.ac.ru

† troitsky@theory.sinp.msu.ru

ber of low-energy nonperturbative models, provided some phenomenological parameters are tuned. In most cases, these models do not attempt to describe the soft-hard transitions (see however a few important exceptions discussed in Sec. IIIB). To our best knowledge, none of the successful low-energy models have described quantitatively and without dedicated tuning of parameters how the asymptotics (1) settles down, given the experimental data. We attempt to do it in the present work.

We start with a well-established Poincaré-invariant constituent-quark model [9–13] which has, for our purposes, the following three advantages:

- (i) **predictivity**: starting from the experimental data on  $F_\pi(Q^2)$  at  $Q^2 \lesssim 0.26 \text{ GeV}^2$  [14], this approach allowed to predict, in 1998, the values of the pion form factor for the extended range of higher momentum transfer [9]. The experimental data obtained later (see Ref. [8] and references therein) for the range of  $Q^2$  larger by an order of magnitude coincide precisely with the prediction of Ref. [9] without any further tuning of parameters;
- (ii) **robustness**: the behaviour of  $F_\pi(Q^2)$  at moderate and high  $Q^2$  does not depend on the selected wave function and is determined by the constituent-quark mass only [9];
- (iii) **asymptotical behaviour**: it has been mathematically proven [15] that in the limit  $Q^2 \rightarrow \infty$  and the constituent-quark mass  $M \rightarrow 0$ , the QCD asymptotical behaviour,  $Q^2 F_\pi(Q^2) \sim \text{const}$ , is obtained in this model.

The points (ii), (iii) suggest a following concept [12, 16] to study the soft-hard transition for  $F_\pi$ . One should adopt the successful low-energy framework and supplement it with a  $Q^2$ -dependent quark mass  $M$ , which should be equal to a constituent-quark mass at  $Q^2 \rightarrow 0$  but should fall at  $Q^2 \rightarrow \infty$  to provide the correct  $M \rightarrow 0$  limit. In this work, we accept a dependence of  $M(Q^2)$  motivated by other studies and fulfill this program.

As a result, we obtain a quantitative description of the hard-soft transition. We will see that, given the experimental data, this transition should not take place at low  $Q^2$ . Therefore, the data on  $F_\pi$  constrain possible models for  $M(Q^2)$  and indicate the presence of large nonperturbative contributions to the light quark mass at least up to  $Q^2 \sim 7 \text{ GeV}^2$ .

The rest of the paper is organized as follows. In Sec. II, we formulate and briefly discuss the model we use. In particular, the concept of the relativistic constituent-quark model is given in Sec. II A, together with references to more detailed descriptions. Sec. II B discusses the selected model for  $M(Q^2)$  and puts it in the context of other approaches used in the literature. We proceed with the calculation of the pion form factor in Sec. III, where we first discuss (Sec. III A) parameters of the model, their fixing/constraining, and the remaining freedom. Results for  $F_\pi$ , obtained within these constraints, are presented

and discussed in Sec. III B, where the comparison with other approaches is also given. We briefly conclude in Sec. IV and list some cumbersome formulae in the Appendix.

## II. THE MODEL

### A. The relativistic constituent-quark model

Our method is a version of the instant form of the Poincaré invariant constituent-quark model (PICQM). This model is described in detail in Refs. [9–13]. Briefly, the model is constructed as follows. In the instant form (IF) of the Relativistic Hamiltonian Dynamics (see e.g. Ref. [17]) one considers two non-interacting one-particle states. Then one separates the center-of-mass motion of the system as a whole and, by means of the Wigner-Eckart theorem for the Poincaré group, extracts the reduced matrix elements, that is form factors [18]. To include the interaction, one finds solutions to the Muskhelishvili-Omnes type equations. These solutions represent wave functions of constituent quarks.

It is important to notice that the approach we use differs from the IF *per se* but it was rather fruitfully complemented by the so-called Modified Impulse Approximation (MIA), see Ref. [10]. MIA is constructed by making use of a dispersion-relation approach and removes certain (often quoted) disadvantages of the IF. In particular, our framework is fully relativistic.

The final result for the pion form factor,  $F_\pi(Q^2)$ , is given by a double integral representation,

$$F_\pi(Q^2) = \int d\sqrt{s} d\sqrt{s'} \varphi(k) g_0(s, Q^2, s') \varphi(k'), \quad (2)$$

where  $s = 4(k^2 + M^2)$ ,  $\varphi(k)$  is the PICQM pion wave function and  $g_0(s, Q^2, s')$  is the free two-particle form factor. The latter may be obtained explicitly by the methods of relativistic kinematics and is a relativistic invariant function; its actual form is rather cumbersome and is given in Appendix for reference.

In Eq. (2),

$$\varphi(k) = \sqrt[4]{s} u(k) k$$

and a phenomenological wave function  $u(k)$  is to be supplied. Fortunately, as it has been shown in Ref. [9], the behaviour of the form factor is insensitive to the choice of the wave function provided a phenomenological boundary condition (correct pion charge radius  $\langle r_\pi^2 \rangle^{1/2}$ ) is satisfied and the correct value of the pion decay constant  $f_\pi$  is reproduced. In the present work, we use the power-law type wave function (see e.g. Ref. [19]),

$$u(k) = N (k^2/b^2 + 1)^{-3},$$

where the normalization coefficient  $N = 16\sqrt{2}/\sqrt{7\pi b^3}$  and  $b$  is a phenomenological parameter related to the confinement scale.

Several other wave functions were shown in Refs. [9, 12] to give the same result for the form factor, provided its low-energy behaviour is fixed by fitting the pion charge radius with a single wave-function parameter,  $b$  in our case. The behaviour of  $F_\pi(Q^2)$  at  $Q^2 \gtrsim 1 \text{ GeV}^2$ , given this fit, is completely determined by  $M$ , as it has been demonstrated in Ref. [9] where calculations have been performed for various  $M$  and different wave-function parametrizations.

The asymptotical behaviour of  $F_\pi(Q^2)$  has been studied in Ref. [15] by considering, mathematically, the  $Q^2 \rightarrow \infty$  limit. In this limit, the original model has two essential dimensionful parameters, the quark mass  $M$  and the confinement scale  $b$ . It has been demonstrated that at  $M \rightarrow 0$ , that is  $M \ll b$ , the QCD asymptotical quark-counting rules are reproduced,  $Q^2 F_\pi(Q^2) \rightarrow \text{const.}$  As we will demonstrate below in the present work (Sec. III B) by numerical calculations, the constant of Eq. (1) is also properly reproduced in the  $M \rightarrow 0$  limit. This is a remarkable success of the model.

### B. Model for the effective $M(Q^2)$

To merge the correct low-energy behaviour (which suggests the constituent-quark mass  $M$  of order the confinement scale  $b$ ) with the correct QCD asymptotics (which requires  $M \ll b$  as we have just discussed above), one should describe the transition between the two regimes by means of a momentum-dependent effective quark mass  $M(Q^2)$ . We will now discuss possible approaches to determination of this function and formulate our prescriptions.

Since the current-quark mass  $m$ , a parameter of the QCD lagrangian, experiences the renormalization-group running and is thus scale-dependent, one might be tempted to identify this  $m(Q^2)$  dependence with the one we are seeking for  $M$ . If this were true, the mass  $m$ , when running from large values of  $Q^2$  down to  $Q^2 \sim \Lambda_{\text{QCD}}^2$ , where the QCD coupling becomes really strong, should acquire large non-perturbative corrections which in turn should increase the mass by two orders of magnitude. The renormalization-group equation for  $m$  has the schematic form

$$\frac{dm^2}{d \log Q^2} = m^2 \gamma(\alpha_s),$$

where  $\gamma(\alpha_s)$  does not depend explicitly on  $m$ . For a small  $m$  this indicates a small derivative, so light particles should remain light unless extreme nonperturbative effects blow up  $\gamma(\alpha_s)$ . The latter possibility is in principle possible, and some authors attempted to run  $m(Q^2)$  all the way down to  $Q^2 = 0$  under certain assumptions about non-perturbative renormalization (see e.g. Ref. [20]). The mass  $m(0)$  obtained in this way was significantly lower than the constituent-quark mass  $M$  inferred from phenomenological models. This is not surprising, however, because, as is most clearly stated

in the ‘‘Quark masses’’ review [21] of the Particle Data Group, the constituent-quark masses ‘‘*make sense in the limited context of a particular quark model, and cannot be related to the quark mass parameters of the Standard Model*’’. Therefore, we should consider the  $Q^2$  dependence of the constituent-quark mass  $M$  starting from its infrared value and cannot impose the QCD value of  $m$  as a precise boundary condition for  $M(Q^2)$  defined in a particular model. The function  $M(Q^2)$  should decrease at large  $Q^2$  to reflect fading of non-perturbative effects, but, being defined in a model-dependent way, it should not be identified with  $m$  anywhere.

There are some remarkable approaches to quantifying this non-perturbative mass ‘‘running’’. One is based on the gap equation supplemented by the effective confining propagator for gluons and a one-gluon exchange for constituent quarks [22, 23]. The resulting  $M(Q^2)$  function was obtained numerically in Ref. [23] by means of a solution to a certain integral equation. It depends on the following four parameters: the confinement scale, two infrared dynamical mass scales and  $\Lambda_{\text{QCD}}$ . While all these parameters are of the same order, one should vary all of them to obtain phenomenologically acceptable results.

Another approach to  $M(Q^2)$  is based on the Dyson-Schwinger equations in QCD [24, 25]. It requires assumptions for the behaviour of the strong coupling constant in the non-perturbative domain which might be quantified with introducing several free parameters (cf. five parameters described in Ref. [26]).

Ref. [16] explored varying quark mass  $M(Q^2)$  in the context of a light-front constituent-quark model, the approach close to the one we follow here. They adopted a parametrization

$$M(Q^2) = M_{\text{uv}} + (M_{\text{ir}} - M_{\text{uv}}) \frac{1 + e^{-\mu^2/\lambda^2}}{1 + e^{-(Q^2 - \mu^2)/\lambda^2}} L(Q^2) \quad (3)$$

with  $L(Q^2) \equiv 1$ , which describes a step-like transition from  $M(0) = M_{\text{ir}}$  to  $M(\infty) = M_{\text{uv}}$  at  $Q^2 \sim \mu^2$ , while the parameter  $\lambda$  is responsible for the smoothness of the transition ( $\lambda = 0$  corresponds to a step). Again, this functional form has four parameters. This form has been subsequently used in other studies [27].

We note that changes in free parameters result in considerable variations of the  $M(Q^2)$  profile in any of the frameworks, while evaluation of  $M(Q^2)$  for each set of parameters, which we have to perform multiple times in our approach, represents a serious numerical task if we choose a dynamical model like Refs. [23, 26]. Therefore we, in a way similar to Ref. [16], also choose an ad hoc parametrization (3); however, we modify it by setting

$$L(Q^2) = \frac{1}{1 + \log \frac{Q^2 + \mu^2}{\mu^2}} \quad (4)$$

to better approximate available examples of  $M(Q^2)$  obtained by detailed calculations, as illustrated in Fig. 1. We note that Eq.(4) does not introduce additional free

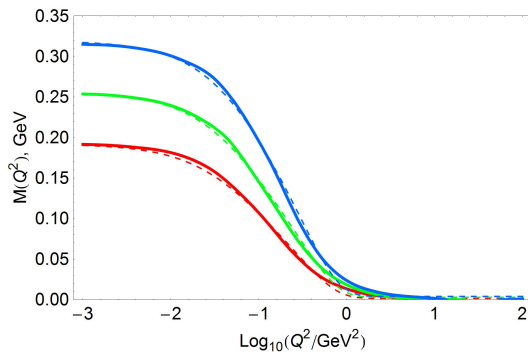


FIG. 1. Comparison of our approximations for  $M(Q^2)$ , Eqs.(3), (4) (dashed lines), with the results of the full calculation of Ref. [23] (thick full lines), for various sets of parameters.

parameters with respect to Eq.(3) but improves significantly the approximation of results of Ref. [23] by imitating the one-gluon-exchange logarithmic contribution.

### III. THE PION FORM FACTOR

#### A. Parameters and constraints

Altogether, the model we use here have the following parameters: the wave-function confinement scale  $b$ ; the infrared and ultraviolet mass asymptotics  $M_{\text{ir}}$ ,  $M_{\text{uv}}$  and the two parameters  $\mu$  and  $\lambda$  which describe the shape of  $M(Q^2)$ , Eqs. (3), (4). As we have discussed above in Sec. II A, the QCD asymptotics requires  $M_{\text{uv}} = 0$ , that is we are left with four parameters<sup>1</sup>. Two of them,  $M_{\text{ir}}$  and  $b$ , correspond to parameters we had in the model with constant  $M$ ; like previously, we tune them to reproduce two observable quantities: the pion decay constant  $f_\pi$  and its charge radius  $\langle r_\pi^2 \rangle^{1/2}$ .

The expression for  $f_\pi$  obtained in Ref. [28],

$$f_\pi = \frac{M\sqrt{3}}{\pi} \int \frac{k^2 dk}{(k^2 + M^2)^{3/4}} u(k), \quad (5)$$

was shown [10] to be valid in our model. The derivation of Eq. (5) implies the zero-momentum limit [10], therefore one should identify  $M = M_{\text{ir}}$  in this formula. We use the most recent Particle Data Group [4] value of  $f_\pi = 130.41 \pm 0.20$  MeV.

The pion charge radius is related to the form factor as

$$\langle r_\pi^2 \rangle^{1/2} = -6 \left. \frac{dF_\pi(Q^2)}{dQ^2} \right|_{Q^2=0}. \quad (6)$$

<sup>1</sup> Numerical instabilities prevent us from taking  $M_{\text{uv}} = 0$  precisely in calculations. All numerical results presented below were obtained for  $M_{\text{uv}} = 3.5 \times 10^{-6}$  GeV. The two additional parameters,  $s_q$  and  $c$ , which describe the departure from the point-quark approximation, cf. Appendix, are taken from the previous studies [10, 12] and kept fixed.

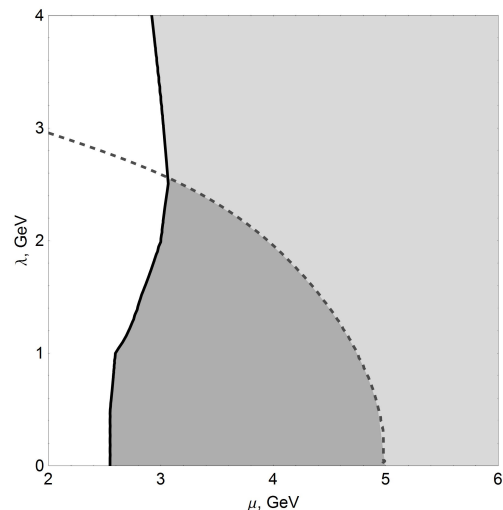


FIG. 2. Constraints on the parameters  $\mu$  and  $\lambda$ . Thick full line is the 95% C.L. limit from the experimental data on  $F_\pi$ ; dashed line is the condition of perturbativity at  $25 \text{ GeV}^2$  (see text). Parameters in the gray region satisfy the experimental constraint; those in the dark-gray region satisfy both.

Hereafter, we use the experimental data on  $F_\pi$  discussed in Ref. [8]. In particular, we exclude some of the early (1976-1978) measurements which, according to Ref. [8], may have large and unknown systematic uncertainties. Since the Particle Data Group world average value of  $\langle r_\pi^2 \rangle^{1/2}$  is strongly affected by these old data, we take instead the most precise value of Ref. [14],  $\langle r_\pi^2 \rangle^{1/2} = 0.663 \pm 0.006$  fm. This is consistent with using the low-momentum data points of Ref. [14] when constraining  $\mu$  and  $\lambda$  as discussed below.

Equations (5) and (6), both related to the  $Q^2 \rightarrow 0$  limit, allow us to fix  $b = 0.6$  GeV and  $M_{\text{ir}} = 0.22$  GeV. Not surprisingly, these values are very close to those used in previous works on the same model ( $M_{\text{ir}}$  is precisely the same while a minor change in  $b$  reflects the change in the world-average value of  $f_\pi$  used). The two parameters  $\mu$  and  $\lambda$  remain unconstrained at this step.

To proceed further, we note that the experimental values of  $F_\pi(Q^2)$  at all momentum transfers covered by the data, that is  $Q^2 \leq 2.45 \text{ GeV}^2$  for the data we use, are in a perfect agreement [8, 12] with the predictions [9] of the model with  $M = \text{const}$ . Given the fact that the behaviour of  $F_\pi(Q^2)$  is determined by  $M$ , see Sec. II A, significant deviations from  $M_{\text{ir}}$  below  $Q^2 \sim 2.5 \text{ GeV}^2$  may spoil the agreement. Therefore, we determine a constraint on  $\mu$  and  $\lambda$  from the agreement with experimental data on  $F_\pi$ , quantified as the 95% confidence-level contour on the  $(\mu, \lambda)$  plane obtained by the standard  $\chi^2$  analysis (Fig. 2). For the determination of this contour, we used the data described in Ref. [8]. These data are presented in Fig. 5 and the references are given in its caption.

This however leaves unconstrained the situation when  $M(Q^2)$  remains large at arbitrary high  $Q^2$ , since the re-

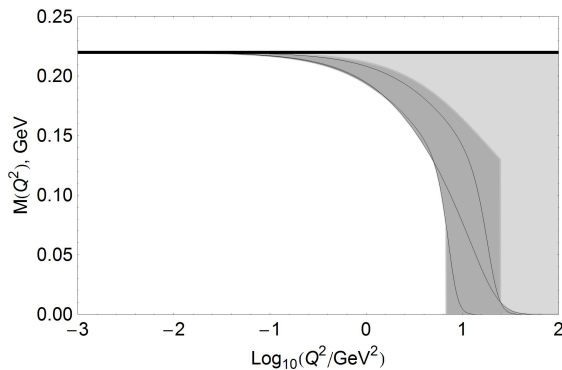


FIG. 3. Examples of  $M(Q^2)$  functions (thin lines) and the full allowed range (gray shadow) determined by the experimental constraints on  $\mu$  and  $\lambda$ . Imposing additional constraint of perturbativity at high  $Q^2$ , see text, restricts the allowed range to the dark-gray region.

sult with  $M = M_{\text{ir}} = \text{const}$  gives an excellent description of the existing data. One may think of an additional, optional constraint on  $(\mu, \lambda)$  related to perturbativity at large  $Q^2$ . Clearly, this condition is qualitative and may be formulated in a number of ways. We note that the recent lattice calculations of the running strong coupling constant (see e.g. Ref. [29]) indicate the agreement with perturbative values at the scales of order 5 GeV and higher. We therefore consider, rather arbitrarily, a condition  $M(Q^2 = 25 \text{ GeV}^2) \lesssim 0.01 \text{ GeV}$ . Neither the precise form nor the very existence of this constraint affect the principal results of this work. This constraint is also shown as a contour on the  $(\mu, \lambda)$  plane in Fig. 2. The allowed range of  $M(Q^2)$  is presented in Fig. 3 together with some examples of the allowed functions.

## B. Results and discussion

The results of the calculation of  $F_\pi$  are presented in Fig. 4. The freedom in the shape of the transition from  $M_{\text{ir}}$  to  $M_{\text{uv}}$  is illustrated by presenting a few example functions  $F_\pi(Q^2)$  corresponding to the  $M(Q^2)$  functions from Fig. 3 which satisfy our constraints. The lower bound on the allowed  $F_\pi(Q^2)$  is determined by the 95% C.L. limit from the present experimental data.

The first and immediate conclusion is that the asymptotics (1) does settle down at  $Q^2 \rightarrow \infty$ , where  $M(Q^2) \approx 0$ . Not only the correct behaviour  $Q^2 F_\pi(Q^2) \simeq \text{const}$  is observed (it was expected from analytical calculations of Ref. [18]), but also the coefficient in Eq. (1) is reproduced numerically, independently of the selected shape of the  $M(Q^2)$  function. This, seemingly miraculous, result indicates a deep connection between low- and high-energy degrees of freedom in our model which will be discussed elsewhere (see however Sec. III G of Ref. [30], an extended version of Ref. [10]).

The second important implication of our results is that the present measurements of  $F_\pi$  constrain the evolution

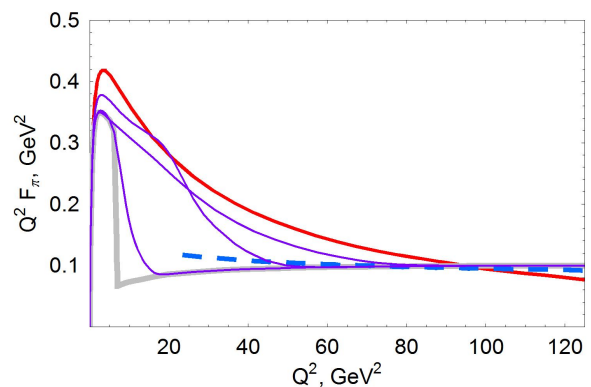


FIG. 4. Examples of the allowed solutions for  $F_\pi(Q^2)$  (thin lines) demonstrating how the QCD asymptotics, Eq.(1) (dashed line) settles down. The thick gray line bounds from below the range of all solutions allowed by the experimental constraints. The thick full (red) line represents the solution with  $M = \text{const}$ , Refs. [9, 12].

of  $M(Q^2)$  far beyond the momentum transfers covered by the data. We see that the effective constituent-quark mass should remain large,  $M \sim \Lambda_{\text{QCD}}$ , at least up to  $Q^2 \sim 7 \text{ GeV}^2 \gg \Lambda_{\text{QCD}}^2$ . Therefore, nonperturbative dynamics is important at these scales and the QCD asymptotics of the pion form factor shall start settling down at even higher values of the momentum transfer.

Let us briefly compare our results with other attempts to describe the transition from soft to hard behaviour of the pion form factor.

A widely used approach to the calculation of the pion form factor, as well as of other observables, is based on the light-front quantization, see Ref. [31]. In particular, it has been applied to the calculation of both soft and hard contributions to the pion form factor more than two decades ago [32]. It was pursued also in Ref. [16], the concept of which is the most close to ours. The authors of Ref. [16], however, did not obtain the asymptotics (1). This fact may be related to properties of the constituent-quark model they used: crucial properties (ii) and (iii) of our model, see Introduction, may not hold for other approaches. An alternative development of the light-front approach is related to holography [33]. The results of Ref. [16] illustrate general trends observed in numerous papers which we cannot review here (see e.g. the review in Ref. [8] and references in [33, 34]): (1) the asymptotics  $Q^2 F_\pi \sim \text{const}$  is not observed and (2) it is difficult to obtain the decrease of  $Q^2 F_\pi$  down to the QCD values and to satisfy the experimental constraints simultaneously. A number of successful approaches therefore give a good description of the data but do not address the high- $Q^2$  behaviour of  $F_\pi$  at all.

The picture similar to what we observe, that is the  $Q^2 F_\pi \sim \text{const}$  behaviour at large  $Q^2$ , has been observed only in Ref. [35], cf. their Fig. 2. The value of the constant obtained in that work may be tuned by changing model parameters within the allowed values. The predic-

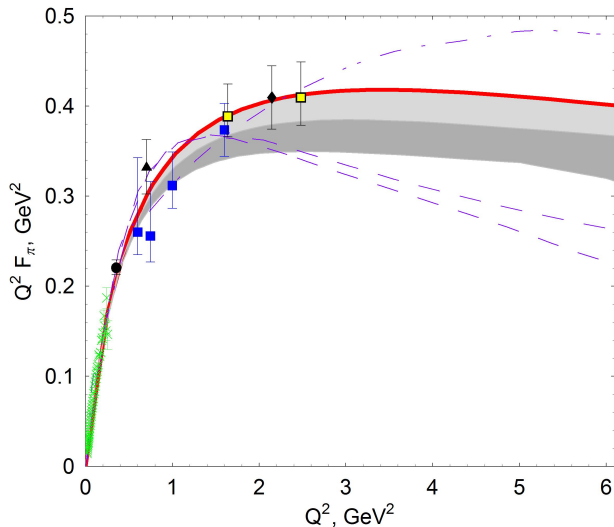


FIG. 5. Predictions of this work for  $F_\pi(Q^2)$  (gray shade; cf. Fig. 3) together with  $M = \text{const}$  prediction of the same model [9, 12] (full line), and those of Refs. [35] (area between two dashed lines) and Ref. [36] (dash-dotted line). The experimental data points from Refs. [14] (crosses), [37] (reanalyzed in Ref. [8], circles), [38] (reanalyzed in Ref. [8], triangles), [39] (diamond) and [8] (squares) are also shown.

tions of Ref. [35] are shown in Fig. 5 together with our results and the experimental data.

Another prediction, which we also plot in Fig. 5, has been obtained in a recent paper [36]. Instead of attempting to reach the asymptotics (1), they choose to calculate corrections to it, which are expected to be large at intermediate values of  $Q^2$ . They note that these corrections (see e.g. Ref. [31]) are related to the pion valence-quark distribution amplitudes  $\phi_\pi(x)$  which differ, at intermediate  $Q^2$ , from their asymptotical values assumed in Eq. (1). They use the non-perturbative information [40, 41] about  $\phi_\pi(x)$  to obtain the corrected asymptotics and predict  $F_\pi(Q^2)$  in a reasonable agreement with it at  $Q^2 \gtrsim 10 \text{ GeV}^2$ . Their approach is complementary to ours: while we start from a constituent-quark model and encode nonperturbative dynamics in  $M(Q^2)$ , they start from QCD and encode nonperturbative dynamics in  $\phi_\pi(x)$ . Note that the perturbative QCD asymptotics, Eq. (1), is not expected to settle down before  $Q^2 > 1000 \text{ GeV}^2$  in their model [36].

From Fig. 5, one can see that different approaches give different predictions for  $F_\pi(Q^2)$  already at  $Q^2 \sim 5 \text{ GeV}^2$ . The expected Jlab upgrade [42] would make it possible to measure the pion form factor at  $Q^2 \leq 6 \text{ GeV}^2$  with the expected precision sufficient to distinguish between the models shown in Fig. 5.

## IV. CONCLUSIONS

This work addresses the pion form factor at intermediate and large momentum transfer. The main result of the paper is twofold.

Firstly, we presented a calculation of  $F_\pi(Q^2)$  for intermediate values of  $Q^2$  and described quantitatively a range of possible scenarios of the soft-hard transition. The calculation has been done in the frameworks of a relativistic constituent-quark model, which had been very successful in predicting the pion form factor behaviour subsequently measured by Jlab. The model was supplemented by a model of effective  $Q^2$ -dependent quark mass motivated by other studies. As a result, we obtained a quantitative description of the transition from the soft constituent-quark regime to the hard QCD asymptotics for the pion form factor. When the quark mass is switched off, the model reproduces the QCD asymptotics (both the  $1/Q^2$  behaviour and the coefficient) of the pion form factor without tuning of parameters, provided the low-energy data are well described.

Secondly, we demonstrated that the existing  $F_\pi$  data indicates that the perturbative QCD fails to describe the pion at momentum transfers at least as large as  $Q^2 \lesssim 7 \text{ GeV}^2$ . In particular, the effective constituent-quark mass does not reach the QCD current-quark running mass at these values of the momentum transfer.

## ACKNOWLEDGMENTS

We are indebted to Stanley Brodsky and Dmitry Levkov for interesting discussions and comments on the draft. ST thanks CERN (PH-TH division) for hospitality at the final stages of this work. The work of ST was supported in part by RFBR (grants 11-02-01528, 12-02-01203, 13-02-01311 and 13-02-01293), the RF President (grant NS-5590.2012.2) and the RF Ministry of Science and Education (agreements 8525 and 14.B37.21.0457).

### Appendix: Formulae for the form-factor calculation

The free two-particle form factor  $g_0(s, Q^2, s')$ , which enters Eq. (2), has the form

$$\begin{aligned}
 g_0(s, Q^2, s') &= \frac{(s + s' + Q^2)Q^2}{2\sqrt{(s - 4M^2)(s' - 4M^2)}} \\
 &\times \frac{\theta(s, Q^2, s')}{[\lambda_1(s, -Q^2, s')]^{3/2}} \frac{1}{\sqrt{1 + Q^2/4M^2}} \\
 &\times \{(s + s' + Q^2)[G_E^q(Q^2) + G_E^{\bar{q}}(Q^2)] \\
 &\times \cos(\omega_1 + \omega_2) + \frac{1}{M} \xi(s, Q^2, s')(G_M^q(Q^2)
 \end{aligned}$$

$$+G_M^{\bar{q}}(Q^2)) \sin(\omega_1 + \omega_2) \},$$

where the notations  $\lambda_1(a, b, c) = a^2 + b^2 + c^2 - 2(ab + ac + bc)$  and

$$\xi = \sqrt{ss'Q^2 - M^2\lambda_1(s, -Q^2, s')},$$

are introduced;  $\omega_1$  and  $\omega_2$  are the Wigner rotation parameters,

$$\omega_1 = \arctan \frac{\xi(s, Q^2, s')}{M[(\sqrt{s} + \sqrt{s'})^2 + Q^2] + \sqrt{ss'}(\sqrt{s} + \sqrt{s'})},$$

$$\omega_2 = \arctan \frac{\alpha(s, s')\xi(s, Q^2, s')}{M(s + s' + Q^2)\alpha(s, s') + \sqrt{ss'}(4M^2 + Q^2)},$$

$\alpha(s, s') = 2M + \sqrt{s} + \sqrt{s'}$ ,  $\theta(s, Q^2, s') = \vartheta(s' - s_1) - \vartheta(s' - s_2)$ ,  $\vartheta$  is the step function,

$$s_{1,2} = 2M^2 + \frac{1}{2M^2}(2M^2 + Q^2)(s - 2M^2)$$

$$\mp \frac{1}{2M^2} \sqrt{Q^2(Q^2 + 4M^2)s(s - 4M^2)}.$$

The functions  $G_{E,M}^{u,\bar{d}}(Q^2)$  are the electric and magnetic form factors of quarks, respectively:

$$G_E^q(Q^2) = |e_q|f_q(Q^2),$$

$$G_M^q(Q^2) = (|e_q| + \kappa_q)f_q(Q^2),$$

where  $q$  denotes the  $u$  and  $\bar{d}$  quarks,  $e_q$  are their charges,  $\kappa_q$  are quark anomalous magnetic moments (that, in the end, enter our calculation through their sum  $s_q = \kappa_u + \kappa_{\bar{d}} \approx 0.0268$ );

$$f_q(Q^2) = \frac{1}{1 + \ln(1 + \langle r_q^2 \rangle Q^2 / 6)},$$

and the quark mean-square radius  $\langle r_q^2 \rangle \approx c/M^2$  with  $c = 0.3$ .

- 
- [1] G. R. Farrar and D. R. Jackson, Phys. Rev. Lett. **43** (1979) 246.
- [2] A. V. Efremov and A. V. Radyushkin, Phys. Lett. B **94** (1980) 245.
- [3] G. P. Lepage and S. J. Brodsky, Phys. Lett. B **87** (1979) 359.
- [4] J. Beringer *et al.* [Particle Data Group Collaboration], Phys. Rev. D **86** (2012) 010001.
- [5] V. A. Matveev, R. M. Muradyan and A. N. Tavkhelidze, Lett. Nuovo Cim. **5** (1972) 907.
- [6] S. J. Brodsky and G. R. Farrar, Phys. Rev. Lett. **31** (1973) 1153.
- [7] A. P. Bakulev, A. V. Pimikov and N. G. Stefanis, Mod. Phys. Lett. A **24** (2009) 2848 [arXiv:0910.3077 [hep-ph]].
- [8] G. M. Huber *et al.* [Jefferson Lab Collaboration], Phys. Rev. C **78** (2008) 045203 [arXiv:0809.3052 [nucl-ex]].
- [9] A. F. Krutov and V. E. Troitsky, Eur. Phys. J. C **20** (2001) 71 [hep-ph/9811318].
- [10] A. F. Krutov and V. E. Troitsky, Phys. Rev. C **65** (2002) 045501 [hep-ph/0204053].
- [11] A. F. Krutov and V. E. Troitsky, Phys. Rev. C **68** (2003) 018501 [hep-ph/0210046].
- [12] A. F. Krutov, V. E. Troitsky and N. A. Tsirova, Phys. Rev. C **80** (2009) 055210 [arXiv:0910.3604 [nucl-th]].
- [13] A. F. Krutov and V. E. Troitsky, Phys. Part. Nucl. **40** (2009) 136.
- [14] S. R. Amendolia *et al.* [NA7 Collaboration], Nucl. Phys. B **277** (1986) 168.
- [15] A. F. Krutov and V. E. Troitsky, Theor. Math. Phys. **116** (1998) 907 [Teor. Mat. Fiz. **116** (1998) 215].
- [16] L. S. Kisslinger, H. -M. Choi and C. -R. Ji, Phys. Rev. D **63** (2001) 113005 [hep-ph/0101053].
- [17] B. D. Keister and W. N. Polyzou, Adv. Nucl. Phys. **20** (1991) 225.
- [18] A. F. Krutov and V. E. Troitsky, Theor. and Math. Phys. **143** (2005) 704 [hep-ph/0412027].
- [19] S. J. Brodsky and F. Schlumpf, Prog. Part. Nucl. Phys. **34** (1995) 69 [hep-ph/9412221].
- [20] A. P. Szczepaniak and E. S. Swanson, Phys. Rev. D **55** (1997) 1578 [hep-ph/9609525].
- [21] A. V. Manohar and C. T. Sachrajda, in Ref. [4].
- [22] J. M. Cornwall, Phys. Rev. D **83** (2011) 076001 [arXiv:1011.3524 [hep-ph]].
- [23] A. Doff, F. A. Machado and A. A. Natale, Annals Phys. **327** (2012) 1030 [arXiv:1106.2860 [hep-ph]].
- [24] C. D. Roberts and A. G. Williams, Prog. Part. Nucl. Phys. **33** (1994) 477 [hep-ph/9403224].
- [25] P. C. Tandy, Prog. Part. Nucl. Phys. **39** (1997) 117 [nucl-th/9705018].
- [26] P. Maris and P. C. Tandy, Phys. Rev. C **62** (2000) 055204 [nucl-th/0005015].
- [27] H. -M. Choi and C. -R. Ji, Phys. Rev. D **74** (2006) 093010 [hep-ph/0608148].
- [28] W. Jaus, Phys. Rev. D **44** (1991) 2851.
- [29] B. Blossier *et al.*, Phys. Rev. Lett. **108** (2012) 262002 [arXiv:1201.5770 [hep-ph]].
- [30] A. F. Krutov and V. E. Troitsky, hep-ph/0101327.
- [31] G. P. Lepage and S. J. Brodsky, Phys. Rev. D **22** (1980) 2157.

- [32] O. C. Jacob and L. S. Kisslinger, Phys. Rev. Lett. **56** (1986) 225.
- [33] S. J. Brodsky and G. F. de Teramond, Phys. Rev. D **77** (2008) 056007 [arXiv:0707.3859 [hep-ph]].
- [34] M. Belicka, S. Dubnicka, A. Z. Dubnickova and A. Liptaj, Phys. Rev. C **83** (2011) 028201 [arXiv:1102.3122 [hep-ph]].
- [35] P. Maris and C. D. Roberts, Phys. Rev. C **58** (1998) 3659 [nucl-th/9804062].
- [36] L. Chang, I. C. Cloet, C. D. Roberts, S. M. Schmidt and P. C. Tandy, arXiv:1307.0026 [nucl-th].
- [37] H. Ackermann *et al.*, Nucl. Phys. B **137** (1978) 294.
- [38] P. Brauel *et al.*, Z. Phys. C **3** (1979) 101.
- [39] T. Horn *et al.*, Phys. Rev. C **78** (2008) 058201 [arXiv:0707.1794 [nucl-ex]].
- [40] I. C. Cloet, L. Chang, C. D. Roberts, S. M. Schmidt and P. C. Tandy, Phys. Rev. Lett. **111** (2013) 092001 [arXiv:1306.2645 [nucl-th]].
- [41] L. Chang *et al.*, Phys. Rev. Lett. **110** (2013) 132001 [arXiv:1301.0324 [nucl-th]].
- [42] J. Dudek *et al.*, Eur. Phys. J. A **48** (2012) 187 [arXiv:1208.1244 [hep-ex]].